Parkinsonism and Related Disorders 20 (2014) 1004–1008

Contents lists available at ScienceDirect

Parkinsonism and Related Disorders

journal homepage: www.elsevier.com/locate/parkreldis

Reduced thalamic volume in Parkinson disease with REM sleep behavior disorder: Volumetric study

M. Salsone [b, 1], A. Cerasa [c, 1], G. Arabia [a], M. Morelli [a], A. Gambardella [a], L. Mumoli [a], R. Nisticò [c], B. Vescio [c], A. Quattrone [a, c, *]

[a] Institute of Neurology, Department of Medical Sciences, University Magna Graecia, Germaneto, Catanzaro, Italy
[b] Neuroimaging Research Unit, National Research Council, Catanzaro, Italy
[c] Neuroimaging Research Unit, Institute of Bioimaging and Molecular Physiology, National Research Council, Germaneto, Catanzaro, Italy

ARTICLE INFO

Article history:
Received 24 February 2014
Received in revised form
16 May 2014
Accepted 17 June 2014

Keywords:
Parkinson disease
REM sleep behavior disorder
Resonance imaging
Voxel-based morphometry
Automated segmentation method

ABSTRACT

Introduction: REM sleep behavior disorder (RBD) is a common non motor feature of Parkinson's Disease (PD) affecting about half the patients with this disease. Distinct structural brain tissue abnormalities have been reported in several regions modulating REM sleep of the patients with idiopathic RBD. At the present time, there are no conventional MRI studies investigating patients with PD associated with RBD.
Methods: Herein, we used voxel-based morphometry (VBM) to detect the neuroanatomical profile of PD patients with and without RBD. Optimized VBM was applied to the MRI brain images in 11 PD patients with RBD (PD-RBD), 11 PD patients without RBD (PD) and 18 age-and sex-matched controls. To corroborate VBM findings we used automated volumetric method (FreeSurfer) to quantify subcortical brain regions volumes. Patients and controls also underwent DAT-SPECT and cardiac MIBG scintigraphies.
Results: The VBM analysis showed markedly reduced gray matter volume in the right thalamus of PD-RBD patients in comparison with PD patients and controls. Automatic thalamic segmentation in PD-RBD patients showed a bilaterally reduced thalamic volume as compared with PD patients or controls. All PD patients (with and without RBD) showed a reduced tracer uptake on DAT-SPECT and cardiac MIBG scintigraphies as compared to controls.
Conclusions: Our findings suggest that the presence of RBD symptoms in PD patients is associated with a reduced thalamic volume suggesting a pathophysiologic role of the thalamus in the complex circuit causing RBD.

1. Introduction

Parkinson's disease (PD) is a progressive neurodegenerative disorder clinically characterized by a core motor features including, akinesia, rigidity and tremor. PD is also associated with non motor symptoms as hyposmia and several sleep disorders including REM sleep behavior disorder (RBD), a parasomnia characterized by dream-enacting behaviors and loss of atonia during the REM sleep. The prevalence of RBD symptoms in patients with PD based on clinical history varies from 15% to 46% while it is estimated in the range between 46% and 58% when the clinical diagnosis of RBD is confirmed using video-polysomnography. In patients with PD exhibiting RBD this parasomnia precedes the onset of parkinsonism in 18–22% of the cases [1].

There is increasing evidence that the presence of RBD in PD patients identifies a clinical subtype of the disease. Indeed, in patients with PD, RBD is associated with older age, longer disease duration [1], rigid-akinetic form of PD and more severe parkinsonian symptoms [2]. These patients may also have increased autonomic dysfunction and higher risk to develop dementia and therefore worse prognosis [3]. Although the clinical phenotype of patients with PD associated with RBD is well known remain still uncertain why only a subset of PD patients develop RBD.

Voxel-based morphometry (VBM) is a well-known unbiased quantitative MR imaging (MRI) method that provides an objective measure of gray and white matter volume changes across the entire brain. Recently, a VBM study [4] conducted in patients with idiopathic RBD (iRBD) showed a significant increase of gray matter density in both hippocampi whereas an other VBM study [5] revealed a significant gray matter reduction in the cerebellum,

* Corresponding author. Institute of Neurology, Department of Medical Sciences, University "Magna Graecia", 88100 Germaneto, Catanzaro, Italy. Tel.: +39 0961 3647075; fax: +39 0961 3647177.
E-mail address: quattrone@unicz.it (A. Quattrone).
[1] These authors contributed equally to this work.

http://dx.doi.org/10.1016/j.parkreldis.2014.06.012
1353-8020/

tegmental portion of the pons and parahippocampal gyrus. Taken together, these findings suggest that many structures with different VBM pattern may be involved in the complex circuit causing RBD.

Several studies have recently validated the use of automated volumetric methods such as FreeSurfer to quantify cortical and subcortical volumes. FreeSurfer calculates brain sub-volumes by assigning a neuroanatomical label to label to each voxel in an MRI volume on the basis of probabilistic information estimated automatically from a manually labeled training set [6].

To our knowledge, there are no conventional MRI reports investigating PD patients associated with RBD. Owing to this lack of investigation, the purpose of the current study was to detect the neuroanatomical profile of PD patients with and without RBD using combined VBM and FreeSurfer analyses.

2. Patients and methods

A total of 11 patients with PD associated with RBD (PD-RBD) and 11 patients with PD without RBD (PD) were recruited from the Neurology Unit of the University "Magna Graecia" of Catanzaro. All subjects met the UK Parkinson's Disease Society Brain Bank clinical diagnostic criteria [7] for PD. DAT-SPECT imaging and cardiac MIBG scintigraphy were also performed in all patients to support a degenerative parkinsonian condition [8]. In all PD patients the RBD symptoms were assessed using the RBD Single-Question Screen [9] (RBD 1Q) a single "yes-no" question that queries the classic dream enactment behavior of RBD. We also performed in all PD patients (with and without RBD) an audio-visual polysomnography (PSG) to confirm the clinical diagnosis of RBD symptoms in PD-RBD group and exclude their presence in PD group. On PSG, a prominent muscle activity in REM sleep associated with abnormal behaviors was required to confirm the clinical diagnosis of RBD [10].

Exclusion criteria were: 1) current treatment with medications know modify REM sleep architecture and muscle tone as serotonin reuptake inhibitors; 2) evidence of structural abnormalities in the brain affecting the gray matter; 3)head movement artifacts during the MRI section; 4) evidence of global cognitive impairment (MMSE $\geq$26) [11]. Before MRI examination, patients underwent a careful clinical assessment including Hoehn-Yahr (H–Y) staging [12] Unified Parkinson's Disease Rating scale (UPDRS) scores [13] and neuropsychological evaluation including MMSE, verbal fluency, token test, Frontal Assessment Battery (FAB) and Back Depression Inventory. Patients were compared to eighteen age-and sex-matched control subjects who had no history suggestive of RBD or other neurological or psychiatric diseases and showed normal MRI of the brain, both normal DAT-SPECT and cardiac MIBG scintigraphy.

3. Magnetic resonance imaging

Brain MRI was performed according to our routine protocol by a 3 T scanner with an 8-channel head coil (Discovery MR-750, GE, Milwaukee, WI, USA). Structural MRI data were acquired using a 3D T1-weighted spoiled gradient echo (SPGR) sequence with the following parameters: TR: 3.7 ms, TE: 9.2 ms, flip angle 12°, voxel-size $1 \times 1 \times 1$ mm^3. Subjects were positioned to lie comfortably in the scanner with a forehead-restraining strap and various foam pads to ensure head fixation.

4. Voxel-based morphometry

Data were processed and examined using the SPM8 software (Wellcome Trust Centre for Neuroimaging, London, UK), where we applied VBM implemented in the VBM8 toolbox (http://dbm.neuro.uni-jena.de/vbm.html) with default parameters incorporating the DARTEL toolbox that was used to obtain a high-dimensional normalization protocol. Images were bias-corrected, tissue classified, and registered using linear (12-parameter affine) and non-linear transformations (warping), within a unified model [14]. Subsequently, the warped gray matter (GM) segments were affine transformed into Montreal Neurological Institute (MNI) space and were scaled by the Jacobian determinants of the deformations (modulated GM volumes). Finally, the modulated volumes were smoothed with a Gaussian kernel of 8 mm full width at half maximum (FWHM). The GM volume maps were statistically analyzed using the general linear model based on Gaussian random field theory. Statistical analysis consisted of an analysis of covariance (AnCOVA) used for investigating the main effect of group (*F*-test). The advantage of an SPM-related F-statistic is that increases and decreases of GM volumes are analyzed together to detect morphological changes in three or more groups. Age and total intracranial volume (ICV) were included in the model as covariates of no-interest. Two approaches to statistical threshold maps were applied. First, we applied a conservative approach with a whole-brain statistical threshold correction ($p < 0.05$, family-wise error (FWE)). Second, since that in vivo evidence of GM abnormalities in PD patients with RBD has never been reported, the data were also presented by using a less-stringent, uncorrected threshold ($p < 0.001$, cluster (k) threshold = 10 voxels) to detect subtle morphological changes.

4.1. Automated subcortical volumetry

To corroborate voxel-based findings we further performed automated labeling and quantification of subcortical brain regions volume using FreeSurfer 5.0. The automated procedures for volumetric measures of several deep gray matter structures have been previously described [6,15]. The automated subcortical segmentation performed by FreeSurfer required these steps: Firstly, an optimal linear transform is computed that maximizes the likelihood of the input image, given an atlas constructed from manually labeled images. A non-linear transform is then initialized with the linear one, and the image is allowed to further deform to better match the atlas. Finally, a Bayesian segmentation procedure is performed, and the maximum a posteriori estimate of the labeling is computed. This approach provides advantages similar to manual ROI drawing [6,16] without the potential for rater bias, offering an anatomically accurate rendering of regional volumes. ICV was

Table 1
Demographic and clinical characteristics and neuroimaging features of PD patients and controls.

Variables	PD-RBD ($n = 11$)	PD ($n = 11$)	Controls ($n = 18$)	*P*-value
Age (y)	66.6 ± 7.4	66.9 ± 7.9	65.1 ± 7.8	0.79[a]
Sex (m/w)	8/3	8/3	13/5	
Age at onset (y)	61.9 ± 6.4	62.5 ± 7.27	–	0.83[b]
Disease duration (y)	4.72 ± 4.07	4.36 ± 4.2	–	0.69[c]
Hoehn and Yahr (HY) stage	1.95 ± 0.57	1.86 ± 0.59	–	0.64[c]
UPDRS	30 ± 15.4	28.9 ± 10.9	–	0.85[b]
UPDRS-ME	21.6 ± 10.4	19.9 ± 10.3	–	0.70[b]
Levodopa dosage (mg/die)	563.6 ± 167.3	547.7 ± 155.4	–	0.92[c]
Rigid-akinetic form (*n*)	3/11	2/11	–	
Onset of RBD symptoms (y)	2.95 ± 1.09			
Cognitive data				
MMSE	27.4 ± 2.87	26.9 ± 3.27	27.9 ± 1.85	0.86[d]
Verbal fluency	24.4 ± 8.77	24.6 ± 12.0	27.2 ± 7.38	0.65[a]
Token test	30.4 ± 5.03	29.5 ± 2.08	31.0 ± 1.88	0.14[d]
F.A.B.	13.6 ± 1.98	14.3 ± 2.36	15.2 ± 1.74	0.09[a]
Beck depression inventory	7.45 ± 4.01	7.54 ± 3.72	6.50 ± 6.89	0.31[d]
DAT-SPECT				
Put/Cau right	1.70 ± 0.22	1.66 ± 0.21	2.46 ± 0.09	<0.001[a]
Put/Cau left	1.73 ± 0.19	1.64 ± 0.19	2.45 ± 0.11	<0.001[a]
Cardiac MIBG scintigraphy				
H/M ratio of delayed images	1.17 ± 0.15	1.14 ± 0.43	1.98 ± 0.10	<0.001[d]

Data are given as mean values (SD) or median range when appropriate.
[a] ANOVA + pairwise *t*-test (with Bonferroni correction).
[b] *t*-test.
[c] Mann–Whitney *U*-test.
[d] Kruskal–Wallis + pairwise Mann–Whitney *U*-test (with Bonferroni correction).

calculated and used to correct the regional brain volumes measurements. Normalized volumetric values were calculated as follows: [raw volume/ICV]*1000. Statistical difference was detected using an AnCOVA model, including age and sex as confounding variables.

4.2. Standard protocol approvals, registrations and patients consents

Before inclusion in the study, written informed consent was obtained from all participants and the study was approved by the institutional review board.

4.3. Statistical analysis

The sex distribution among all groups and the form distribution in PD and PD-RBD patients were compared using Fisher's exact test. Differences in age at examination, Put/Cau right and Put/Cau left, verbal fluency and FAB among groups were assessed using the one-way analysis of variance (ANOVA), followed by pairwise *t*-tests with Bonferroni correction. The unpaired *t*-test was used to assess differences in age at onset, UPDRS and UPDRS-ME scores. The Mann–Whitney *U*-test was used to compare age at onset and Hoehn-Yahr scores between PD and PD-RBD groups of the patients. Differences in cardiac MIBG scintigraphy and MMSE, Token Test and Beck scores were assessed using the Krukal–Wallis rank sum test followed by pairwise Mann–Whitney *U*-tests, with *p*-values corrected according to Bonferroni. All tests were two-tailed, and the α-level was set at $p = 0.05$. Statistical analysis was performed with R Statistical Software (R for Unix/Linux, version 2.11.1, The R Foundation for Statistical Computing, 2010).

5. Results

There was no significant difference in demographic and clinical data between PD-RBD and PD groups of patients as shown in Table 1. PD patients showed a marked decrease of the tracer uptake in both DAT and MIBG scintigraphies (Table 1). Levodopa

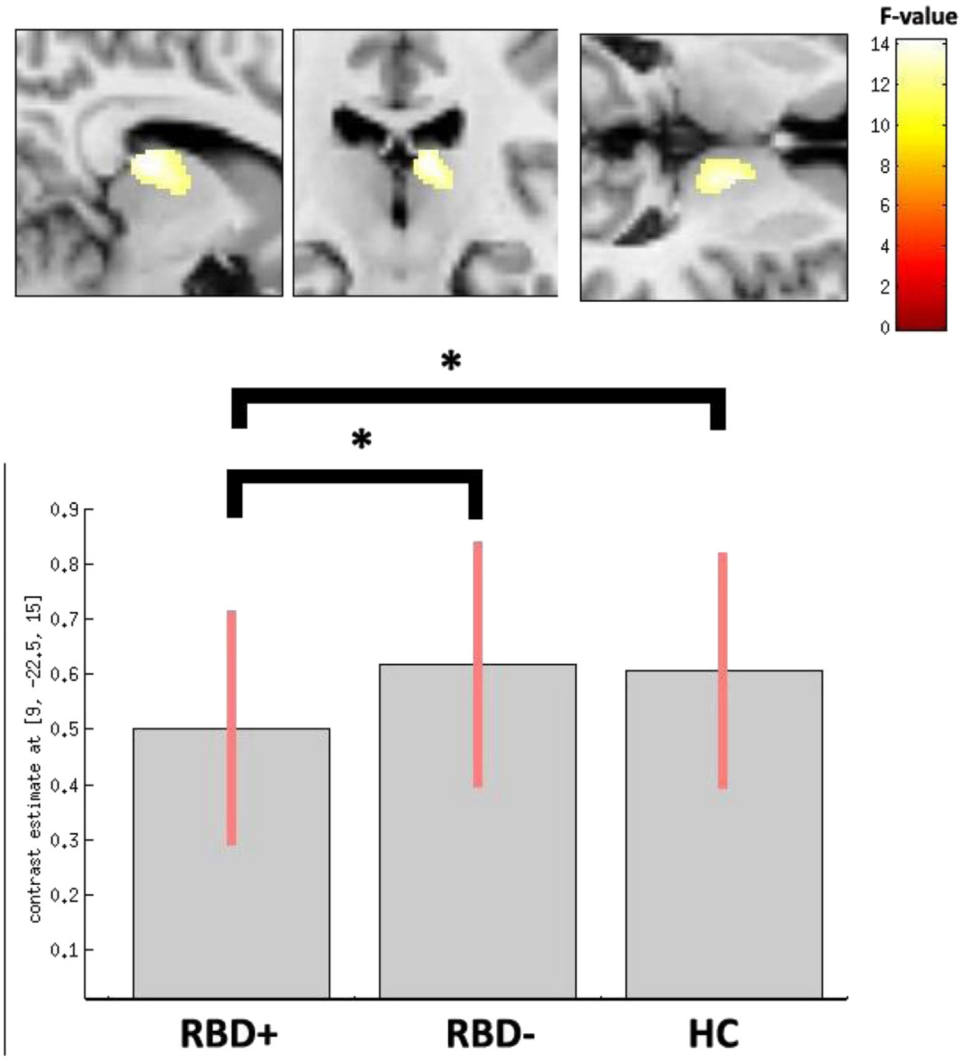

Fig. 1. VBM results. 2D surface render shows the significant cluster deriving from the main effect of group. Significant difference (surviving correction for multiple comparisons at a whole brain level, FWE < 0.05) is found only in the right thalamus, where patients having PD-RBD display an abnormal decrease of the GM volume with respect to other groups. Mean differences (±SEM) between groups within region of statistical significance have been plotted below. Statistical map is superimposed onto the T1-weighted standard template (MNI). Data analyses have been further corrected for age and intracranial volume. The color bar represents F-statistics. RBD+: PD patients affected by REM sleep behavior disorder; RBD−: PD patients without REM sleep behavior disorder; HC Healthy Controls.

dosage was not significantly different between two PD groups (Table 1). VBM analysis, investigating the neuroanatomical changes occurring when the 3 groups were analyzed together (AnCOVA, *F*-test), revealed the presence of a very restrict pattern of difference surviving correction for multiple comparisons at a whole brain (FWE < 0.05). As shown in Fig. 1, VBM analysis revealed a significant decrease of gray matter volume in the right thalamus (MNI local maxima: $x = -9$, $y = -21$, $z = 15$, *F*-value = 14.16; (k) = 85 PFWE < 0.04) in PD-RBD patients as compared to PD patients without RBD and controls. For exploratory purpose, we also reported volumetric changes occurring when a less-stringent uncorrected statistical threshold was considered (Puncorrected < 0.001). Patients with PD-RBD showed additional gray matter abnormalities in the right medial temporal cortex (MNI local maxima: $x = 68$, $y = -22$, $z = -6$, *F*-value = 11.86, (k) = 176 Puncorrected < 0.001) whereas PD patients did not show evidence of significant morphological abnormalities. In PD-RBD patients, we also detected some gray matter changes in the brainstem only decreasing statistical threshold to a level that is statistically not acceptable ($p < 0.05$ uncorrected) in comparison to PD patients.

To further corroborate VBM findings, we performed automatic thalamic segmentation using FreeSurfer. PD-RBD patients were characterized by reduced volume of the right thalamus ($F_{2,36} = 5.9$; p-level = 0.006) either when compared to PD patients (post-hoc *t*-test; *p*-level = 0.004) or controls (post-hoc *t*-test; p-level = 0.003) (Fig. 2). Automated volumetry revealed also a significant gray matter loss of the left thalamus ($F_{2,36} = 3.5$; *p*-level < 0.03), which resulted to be only driven by the direct comparison between PD groups (post-hoc *t*-test; *p*-level = 0.03).

6. Discussion

The current study provides the first in vivo evidence of structural brain abnormalities in PD patients associated with RBD symptoms. Indeed, we found a significant decrease of the thalamic volume in PD-RBD patients in comparison with PD patients using combined voxel-based morphometry and volumetric MRI techniques.

Previous imaging studies investigated the brain tissue changes in patients with iRBD. A recent combined Diffusion Tensor Imaging and VBM study [4] revealed a significant increase of gray matter density in both hippocampi whereas an other VBM study [5] showed a significant gray matter reduction in the cerebellum, tegmental portion of the pons and parahippocampal gyrus, suggesting that many structures with different VBM pattern might be involved in the complex circuit causing RBD. However, all MRI studies reported were performed in patients with iRBD who could have different pathophysiological mechanism from those involved in PD-RBD.

RBD is likely caused by neuronal dysfunction in the brain regions that regulate the suppression of skeletal muscle tone during REM sleep. There is converging evidence that the dysfunction of brainstem cholinergic and monoaminergic neurons may be of importance in the pathogenesis of this behavioral disorder. Component of this complex circuit include the cholinergic nucleus peduncolopontine (PPN) and the lateral dorsal tegmental nuclei (LDTN), the serotonergic raphe nucleus, and the glutamatergic and monoaminergic projections from subcoeruleus/coeruleus region [17]. During REM sleep, the ascending neurons from subcoeruleus/

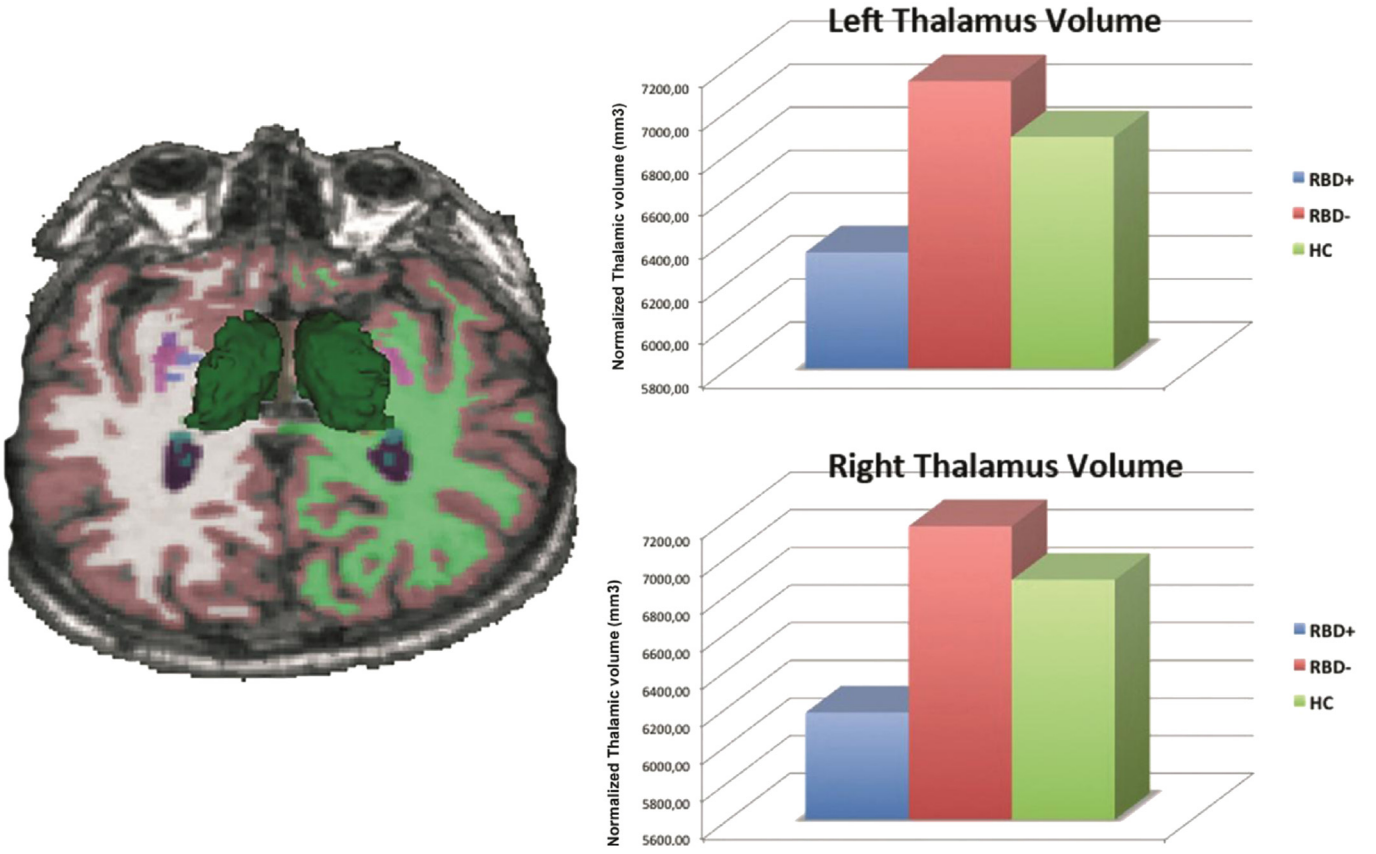

Fig. 2. Sample color-coded subcortical segmentation results. 3D surface models, created with 3D Slicer, Version 3 (www.slicer.org), are derived from the FreeSurfer subcortical segmentation of the thalamus (green). Significant volumetric differences were detected between PD patients with RBD (blue bar) with respect to PD patients without RBD (red bar) and healthy controls (green bar). Bar plots of the mean normalized volumes of the left and right thalamus for each single group has been plotted on the right side.

coeruleus region in collaboration with cholinergic neurons originating in the PPN and LDNT excite intralaminar thalamocortical neurons which in turn activate the cortex [18,19]. Supporting the concept of functional interaction between cholinergic PPN-LDNT and thalamus, it was recently reported that in PD patients with RBD the dysfunction of PPN-LDTN might cause a diminished thalamic cholinergic innervation. Moreover, this recent PET study has demonstrated that the presence of RBD symptoms in PD is associated with thalamic cholinergic denervation as a consequence of brainstem degeneration [17].

In accordance with these findings, more recently, some authors [20] have found a significant decrease in the signal intensity in the coeruleus/subcoeruleus complex in PD-RBD patients in comparison with PD without RBD and controls using combined neuromelanin-sensitive structural and diffusion MRI techniques. These authors, however, did not report any significant difference in gray and white matter volumes between subgroups of PD patients (with and without RBD) probably because their MRI analyses were limited to the brainstem.

Neuropathological studies [21–23] have confirmed the involvement of thalamic nuclei in RBD demonstrating that the thalamus is a key structure in Lewy body diseases being one of the select targets of extranigral inclusion body pathology. The thalamus accumulates α-synuclein inclusions which mainly concentrate in the intralaminar [21] and limbic system nuclei [22]. Thalamic Lewy body pathology was recently found to be more pronounced also in PD cases with sleep disturbances including RBD as compared with PD without sleep disturbances [23].

In accordance with these previous studies, our study demonstrated a reduced thalamic volume in PD patients associated with RBD symptoms. Indeed, VBM analysis revealed a significant decrease of gray matter volume in the right thalamus of PD-RBD patients as compared to PD patients without RBD and controls. In particular, we can hypothesize that the structural abnormalities we found only in the right thalamus on VBM analysis were due to the highly stringent statistical threshold (FEW<0.05) employed in a small number of patients. This hypothesis was further supported by automatic thalamic segmentation which showed a reduced volume of both left and right thalami in PD-RBD as compared with PD patients and controls.

Taken all together, these findings suggest that thalamus may play a role in the development of RBD, and that thalamic atrophy reported in our PD-RBD patients may reflect both the accumulation of α-synuclein inclusions which mainly concentrate in the intralaminar nuclei and the loss of input from coeruleus/subcoeruleus to thalamus and cortex, consequent to dysfunction or degeneration of this complex.

There are some limitations to this study. First, we lack pathologic examination and we do not know whether our PD patients (with and without RBD) have or not Lewy body pathology in the brain including thalami. All PD patients, however, had markedly reduced cardiac MIBG uptake, a finding suggestive of Lewy body accumulation in cardiac sympathetic nerve endings [8]. Second, the number of both PD groups of patients is small. Further studies in a larger cohort are warranted.

In summary, our findings suggest that the presence of RBD symptoms in PD patients is associated with a reduced thalamic volume and support the hypothesis of pathophysiologic role of the thalamus in the complex circuit causing RBD.

References

[1] Iranzo A, Santamaria J, Tolosa E. The clinical and pathophysiological relevance of REM sleep behaviour disorder in neurodegenerative diseases. Sleep Med Rev 2009;13:385–401.

[2] Nomura T, Inoue Y, Kagimura T, Nakashima K. Clinical significance of REM sleep behaviour disorder in Parkinson's disease. Sleep Med 2013;14:131–5.

[3] Postuma RB, Gagnon JF, Montplaisir JY. REM sleep behaviour disorder: from dreams to neurodegeneration. Neurobiol Dis 2012;46:553–8.

[4] Scherfler C, Frauscher B, Schocke M, Iranzo A, Gschliesser V, Seppi K, et al. White and gray matter abnormalities in idiopathic rapid eye movement sleep behaviour disorder. Ann Neurol 2011;69:400–7.

[5] Hanyu H, Ionue Y, Sakurai H, Kanetaka H, Nakamura M, Miyamoto T, et al. Voxel-based magnetic resonance imaging study of structural brain changes in patients with idiopathic REM sleep behaviour disorder. Parkinsonism Relat Disord 2012;18:136–9.

[6] Cerasa A, Messina D, Nicoletti G, Novellino F, Lanza P, Condino F, et al. Cerebellar atrophy in essential tremor using an automated segmentation method. AJNR Am J Neuroradiol 2009;30:1240–3.

[7] Huges AJ, Daniel SE, Kilford L, Lees AJ. Accuracy of clinical diagnosis of idiopathic Parkinson's Disease: a clinico-pathological study of 100 cases. J Neurol Neurosurg Psychiatry 1992;55(3):181–4.

[8] Salsone M, Bagnato A, Novellino F, Cascini GL, Paglionico S, Cipullo S, et al. Cardiac MIBG scintigraphy in primary progressive freezing gait. Parkinsonism Relat Disord 2009;15:365–9.

[9] Postuma RB, Arnulf I, Hogl B, Iranzo A, Miyamoto T, Dauvilliers Y, et al. A single-question screen for rapid eye movement sleep behaviour disorder: a multicenter validation study. Mov Disord 2012;27:364–71.

[10] Iranzo A, Aparicio J. A lesson from anatomy: focal brain lesions causing REM sleep behaviour disorder. Sleep Med 2009;10:9–12.

[11] Folstein MF, Folstein SE, McHugh PR. "Mini mental state". A practical method for grading the cognitive state of patients for the clinician. J Psychiatr Res 1975;12:189–98.

[12] Hohen MM, Yahr MD. Parkinsonism: onset, progression and mortality. Neurology 1967;17:427–42.

[13] Fahn S, Elton RL. Unified Parkinson's disease rating scale. In: Fahn SMC, Goldstein M, Calne DB, editors. Recent developments in Parkinson's disease II. New York: MacMillan; 1987. pp. 153–63.

[14] Ashburner J, Friston KJ. Unified segmentation. Neuroimage 2005;26:839–51.

[15] Fischl B, van der Kouwe A, Destrieux C, Halgren E, Ségonne F, Salat DH, et al. Automatically parcellating the human Cerebral Cortex. Cereb Cortex 2004;14:11–22.

[16] Morey RA, Petty CM, Xu Y, Hayes JP, Wagner 2nd HR, Lewis DVA, et al. Comparison of automated segmentation and manual tracing for quantifying hippocampal and amygdala volumes. Neuroimage 2009;45:855–66.

[17] Kotagal V, Albin RL, Muller M, Koeppe RA, Chervin RD, Frey KA, et al. Symptoms of rapid eye movement sleep behaviour disorder are associated with cholinergic denervation in Parkinson Disease. Ann Neurol 2012;71:560–8.

[18] Garcia-Lorenzo D, Longo-Dos Santos C, Ewenczk C, Leu-Semenescu S, Gallea C, Quattrocchi G, et al. The coeruleus/subcoeruleus complex in rapid eye movement sleep behaviour disorders in Parkinson's Disease. Brain 2013;136:2120–9.

[19] Nardone R, Golaszewki S, Holler Y, Ristova M, Trinka E, Brigo F. Neurophysiological insights into the pathophysiology of REM sleep behaviour disorders:a review. Neursci Res 2013;76(3):106–12.

[20] Luppi P-H, Clement O, Garcia S, Brischoux F, Fort P. New aspects in the pathophysiology of rapid eye movement sleep behaviour disorder: the pothential role of glutamate, gamma-aminobutyric acid, and glycine. Sleep Med 2013;4(8):714–8.

[21] Brooks D, Halliday GM. Intralaminar nuclei of the thalamus in Lewy body diseases. Brain Res Bull 2009;78:97–104.

[22] Rub U, Del Tredici K, Schultz C, de Vos RA, Jansen Steur E, Braak H. Parkinson's Disease: the thalamic components of limbic loop are severely impaired by α-synuclein immunopositive inclusion body pathology. Neurobiol Aging 2002;23:245–54.

[23] Kalaitzakis ME, Gentleman SM, Pearce RKB. Disturbed sleep in Parkinson's disease anatomical and pathological correlates. Neuropathol Appl Neurobiol 2013;39(6):644–53.